sciendo INTERNATIONAL JOURNAL ON SMART SENSING AND INTELLIGENT SYSTEMS

Article | DOI: 10.2478/ijssis-2023-0001 Issue 1 | Vol. 16 (2023)

Spatial distribution of soil nutrient content for sustainable rice agriculture using geographic information system and Naïve Bayes classifier

Anton Yudhana[1]*, Andreyan Dwi Cahyo[1], Liya Yusrina Sabila[1], Arsyad Cahya Subrata[1] and Ilham Mufandi[2]

[1]Department of Electrical Engineering, Faculty of Industrial Technology, Universitas Ahmad Dahlan, Unit IV, Jl. Ringroad Selatan, Kragilan, Tamanan, Banguntapan, Bantul Regency, Special Region of Yogyakarta 55191, Indonesia

[2]Department of Agro-industrial Technology, Faculty of Science and Technology, University of Darussalam Gontor, Ponorogo 63471, Indonesia

*E-mail: eyudhana@ee.uad.ac.id

This paper was edited by Subhas Chandra Mukhopadhyay.

Received for publication: June 5, 2022.

Abstract

This study aims to assist farmers in monitoring soil nutrients, especially phosphorus. To measure the phosphorus content of paddy soil, the TCS3200 converter, as an intelligent sensor, was applied. The geographical information system (GIS) was also involved in this research to map the phosphorus content. In addition, the Naïve Bayes method was applied to classify lowland soil phosphorus status. The result of this study indicated that the Naïve Bayes algorithm could classify lowland soil phosphorus status with a probability of 0.34 for moderate phosphorus conditions and 0.66 for high phosphorus conditions. The sample testing results showed that the error rate was 3% and the success rate was 97%. Testing with a phosphorus-measuring instrument can be carried out by mapping the soil phosphorus status with the ArcGIS software, whereby seven points of medium-phosphorus-status paddy soil and 13 locations of high-phosphorus-status soil samples were determined. This research thus successfully mapped the soil phosphorus.

Keywords

Soil phosphorus, TCS3200 sensor, Geographic Information System (GIS), Naïve Bayes

1. Introduction

The agricultural sector is vital for several developing countries in terms of its role in supporting the economy [1], [2]. That is seen that the role of the agricultural sector is to employ the population, create national income, and contribute to gross domestic product [3], [4]. The agricultural sector also offers additional benefits, such as ensuring the quality and stability of the environment(mitigating floods, controlling soil erosion, maintaining the groundwater supply, sequestering carbon, air conditioning and freshening, organic waste recycling, and maintaining biodiversity), preservation of sociocultural values and rural attractiveness (rural amenity), buffering financial stability, alleviating poverty, and various other services [5], [6]. One of the products of the agricultural sector is rice. Rice is a staple food source in Indonesia. The life cycle of the rice plant depends on water availability because water has a vital role in both human life and the rice plant ecosystem [7]–[9]. The quality of the food consumed is influenced by several factors, such as the weather, the content of natural chemical compounds in the food, and the water quality [7], [8], [10], [11]. Rice plants grow excellently in ecosystems having areas with availability of abundant water for irrigation and huge amounts of water vapor [7], [12]. Around 0-1500 mesh is suitable for the rice plant ecosystem [13]. Phosphorus is an essential micronutrient for organisms. Water and soil contain inorganic compounds of phosphorus [14], [15]. Sediment deposition and soil causes phosphate to dissolve in groundwater and seawater [16].

Phosphorus (*P*) is essential for all life on Earth and, for plants, it is a key element in photosynthesis, respiration, and the biosynthesis of nucleic acids and membranes [17]–[19]. It also performs a vital role in regulating many enzymes [20]. As a plant macronutrient, phosphorus frequently limits both natural and agricultural systems [17], [21]. It is a structural and functional component of nucleic acids, membrane lipids, energy metabolites, and activated intermediates within the photosynthetic carbon cycle; moreover, inorganic phosphate (*Pi*) plays an essential role in signal transduction or cellular response for knowing the nutrient in living organisms [22]. Phosphorus has a principal role in stimulating the growth of plant roots and accelerating the growth of flowers into fruits to speed up the harvest period [23]. However, the role of phosphorus in the soil is influenced by soil pH. Alkaline pH levels cause phosphorus to decrease [24]. For maintaining the condition of the soil, fertilizer is added to the soil to increase the nutrient content and improve crop production and quality [25], [26]. However, it affects the accumulation of phosphorus in the soil during irregular fertilization [27]. There is a limitation in the context of monitoring of the quality and content of soil nutrients, which is still done manually by farmers. Advanced science and technology are needed to obtain a better crop yield [28].

One of the methods to increase agricultural production is applying precision farming patterns, specifically by monitoring and analyzing soil conditions [29]–[31]. This research aims to help farmers with fertilizer recommendations with a map of nutrient status based on the geographic information system (GIS) [32]. There are many definitions of geographic information and the systems used to store, retrieve, examine, and show facts that might be represented spatially or geographically [33], [34]. Geographic information can be manipulated or stored using GIS, a computer-based system [35], [36]. In the literature [36]–[38], there are numerous reports on the usage of GIS to make decisions regarding land resources with the aim of reaching an acceptable use of land for optimum food production and profit. One of the key benefits of using GIS is its application for soil evaluation. The presentation of effects can be achieved spatially explicitly in the form of maps to show the spatial distribution of geographic features [34], [39]. GIS implementation is expected to assist farmers in monitoring soil phosphorus content and efficient fertilization processes.

One method that can support mapping of the soil phosphorus content of agricultural rice land-based on GIS is the Naïve Bayes algorithm [40]–[42]. Previous studies [43], [44] have investigated the use of the Naïve Bayes algorithm. The previous work from [43] also predicted landslides based on selected risk factors with an accuracy of 79.8%, whereas another work [44] investigated decision-making regarding the quality of soil with an accuracy of 87.5%. Hence, this work aims to apply phosphorus mapping to paddy soil using the Naïve Bayes method in combination with GIS. This system uses the TCS3200 sensor [45] on 20 samples of lowland soil, which are tested 200 times in Lendah district, Yogyakarta, Indonesia. The sample-testing results show an error rate of 3% and a success rate of 97%. GIS-based mapping results can be used as monitoring data for evaluating the possible phosphorus content in paddy soil.

2. Research Methods

2.1. Paddy Soil Test Kit (PUTS)

This device is accurate, easy, and relatively fast in analyzing the nutrient content in the soil. Nitrogen, phosphorus, potassium, and soil pH are the primary measurement targets for the PUTS design. The Paddy Soil Test Kit (PUTS) kit consists of several chemicals used for extracting soil nutrients, a leaf color chart (BWD), and instructions for use, along with fertilizer recommendations. The image of a PUTS device is shown in Figure 1.

2.2. Naïve Bayes Classifier Algorithm

Probability and statistics are classification methods found in the Naïve Bayes method. This method was proposed by Thomas Bayes and is used as a reference to predict future opportunities based on previous experience [46], [47]. Naïve Bayes Classifier requires a small amount of training data to achieve classification of the parameters. The variables in this method are assumed to determine each class [42]. Naïve Bayes classification is obtained by using the following expression:

$$P(x) = \frac{P(c)P(c)}{P(x)}, \quad (1)$$

where $P(c)$ = class prior probability; $P(x|c)$ = likelihood; $P(x)$ = predictor prior probability; and $P(c|x)$ = posterior probability.

Figure 1: Paddy Soil Test Kit (PUTS).

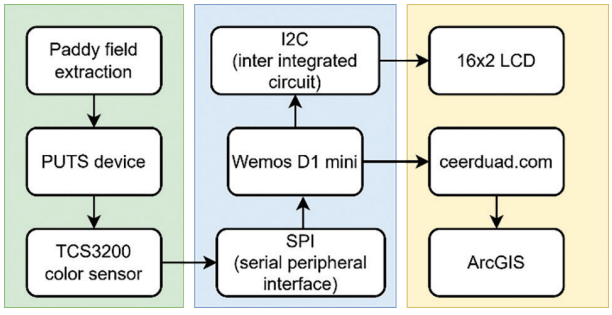

Figure 2: The block diagram of the measurement process of phosphorus using a paddy soil phosphorus meter.

2.3. System Planning

Figure 2 shows the block diagram of this system.

The block diagram in Figure 2 shows the working of the paddy soil phosphorus meter. The initial stage is to get the color of soil phosphorus in the paddy soil samples extracted using PUTS. The Soil phosphorus determination are obtained using the TCS3200 sensor through the serial peripheral interface (SPI) communication line connected to the Wemos D1 Mini board. The resulting data of the TCS3200 sensor are processed on the Wemos D1 Mini board, which is connected to a 5 V voltage source. The data processed on the Wemos board and classified using the Naïve Bayes method are displayed on a 16 × 2 liquid-crystal display (LCD) and then sent to the *ceerduad.com* website. Wemos is used because it is a microcontroller that has an integrated Internet of Things (IoT) system and a wireless fidelity (WiFi) module with 4 MB of storage memory [48]. The data are displayed on a 16 × 2 LCD, and the web map is then created using ArcGIS software.

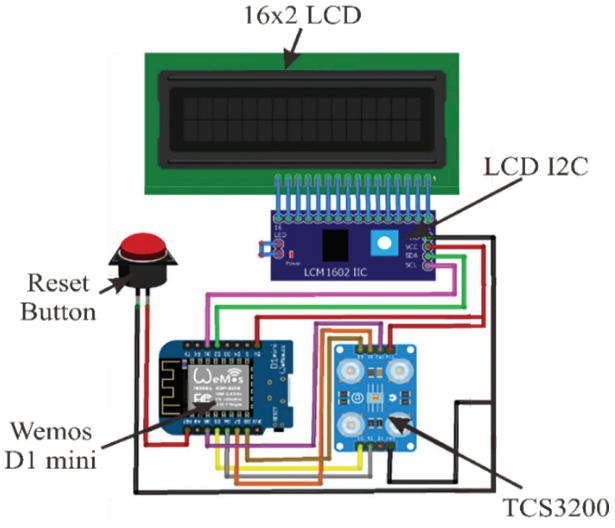

Figure 3: Wemos D1 Mini system series and TCS3200 sensor.

2.4. Hardware Design

The Wemos D1 Mini system control is a WIFI-based development board module designed as a sensor controller. Sensor reading data are processed on the sensor controller. The outline of the series of systems designed for measuring the phosphorus levels in paddy soil is shown in Figure 3.

2.5. Hardware Design of Paddy Soil Phosphorus Measurement System

The design of this measuring instrument program uses Arduino Uno. The program results are then uploaded to the Wemos D1 Mini board. The software design is shown in the flowchart in Figure 4. In the

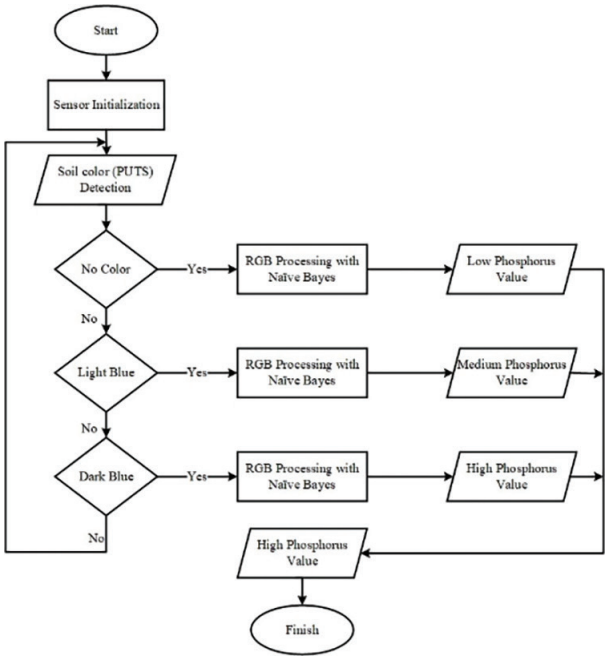

Figure 4: Flowchart of the phosphorus detection program in this system.

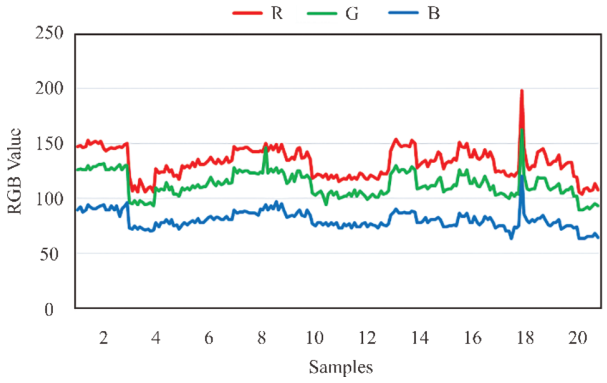

Figure 5: Design of Phosphorus Measurement Tool System.

workflow of this paddy soil phosphorus meter, when the measuring instrument is running, the sensor will immediately read the room value, which will be used as the sensor's default value for calibration. If the calibration is successful, it will display a command to insert the extracted soil sample to read the red, green, and blue (RGB) values. The classification process is carried out with the Naïve Bayes algorithm. The results of the classification process are displayed on the LCD, and the RGB values of the soil samples are sent to *ceerduad.ac.id*, a web server, in the form of low, medium, or high phosphorus status. The design of the phosphorus measurement tool is shown in Figure 5.

3. Results and Discussion

3.1. Determination of Soil Phosphorus Status

From the readings of the phosphorus level obtained using the TCS3200 sensor for the 20 soil samples extracted, this study obtained the RGB values shown in Table 1.

The RGB values in Table 1 constitute the data snippet from the 200 training data used for reading phosphorus levels on the PUTS color chart. For determining the phosphorus level status, 20 soil samples were used, and each soil sample contained 10 training data for sensor readings. The graph of RGB values obtained from these 20 samples is shown in Figure 6. The soil sample measurements produced 200 experimental data values, out of which 194 measurement data obtained using a phosphorus measuring instrument based on PUTS measurements were valid and six experimental results were not suitable. From the results obtained, the error value can be calculated using Eq. (2) as follows:

$$Error = \frac{Numb.\ of\ PUTS\ Tests - Numb.\ of\ Testing\ of\ Measuring}{Numb.\ of\ PUTS\ Tests} \times 100\% \quad (2)$$

$$Error = 3\%$$

Using the Naïve Bayes equation, we found that the error rate of the measuring instrument was 3%, and the instrument accuracy was 97%. This result was compared with previous research that was applied for nitrogen monitoring [44], with an accuracy of 87.5%. To measure the accuracy, other studies used the coefficient of determination (R^2), as shown previously [49] for monitoring of the leaf nitrogen concentration of wheat, with accuracy of 0.91%. Another study [50] calculated the accuracy of the sensor by using the coefficient of determination (R^2) for measuring the total nitrogen content in agricultural runoff. [53] also proposed the monitoring of wheat grain nitrogen content with the coefficient of determination (R^2), with a result of 0.42%.

Table 1. RGB values of the paddy soil sample reading

Sample	Testing	Red	Green	Blue	Proposed system status	PUTS status	Sample	Testing	Red	Green	Blue	Proposed system status	PUTS status
1	1	147	126	90	High	High	11	1	116	100	73	Medium	Medium
	2	148	127	92	High	High		2	117	101	73	Medium	Medium
2	1	145	132	94	High	High	12	1	118	102	78	Medium	Medium
	2	143	126	90	High	High		2	117	99	74	Medium	Medium
3	1	121	96	73	Medium	Medium	13	1	143	122	85	High	High
	2	107	95	72	Medium	Medium		2	150	126	88	High	High
4	1	127	110	78	High	Medium	14	1	128	109	78	High	High
	2	123	107	74	Medium	Medium		2	131	110	78	High	High
5	1	130	110	76	High	High	15	1	127	106	74	High	High
	2	128	108	78	High	High		2	132	108	74	High	High
6	1	135	116	83	High	High	16	1	138	114	78	High	High
	2	138	119	84	High	High		2	138	114	78	High	High
7	1	147	128	90	High	High	17	1	124	103	73	Medium	Medium
	2	144	123	87	High	High		2	125	104	75	Medium	Medium
8	1	143	124	91	High	High	18	1	198	163	120	Medium	Medium
	2	142	123	90	High	High		2	146	121	86	High	High
9	1	135	114	83	High	High	19	1	131	110	76	High	High
	2	135	116	84	High	High		2	131	108	75	High	High
10	1	118	105	77	Medium	Medium	20	1	120	102	73	Medium	Medium
	2	120	103	75	Medium	Medium		2	119	102	74	Medium	Medium

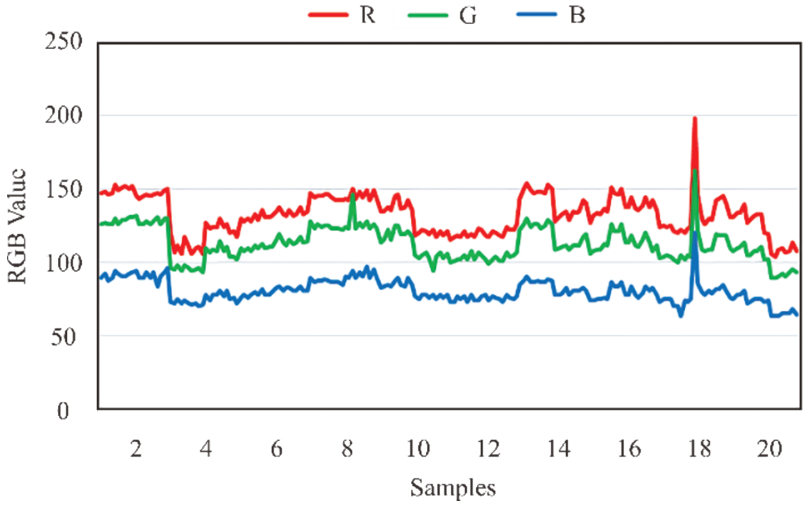

Figure 6: Soil Sample Test.

3.2. Naïve Bayes Analysis

The Naïve Bayes method is used to calculate the probability of an event occurring in the future based on previous experience [51], [52]. Naïve Bayes analysis was used to classify the test results of the 20 soil samples to obtain the paddy soil phosphorus status. Based on the graph in Figure 6, the result obtained was as follows:

$$P\left(c\left(MEDIUM\right)\right) = 68 / 200 = 0.34 \text{ ;}$$

$$P(c(\text{HIGH})) = 132 / 200 = 0.66.$$

Tables 2–4 show the RGB value probabilities from the research results.

Table 2 shows the probability of phosphorus status in each class of red values divided into four ranges (1-63, 64-127, 128-190, and 192-255). Classification results based on red odds indicate the possibility of a medium or high level of phosphorus content. The probability of the green value class is shown in Table 3.

Table 3 shows the probability of the phosphorus status in each green value class divided into four classes with moderate- and high-phosphorus-status probabilities. The RGB reading value ranges from 1 to 255. The probability of the blue value status is shown in Table 4.

Table 4 shows the probability of phosphorus status in each blue value class divided into four classes with moderate and high phosphorus-status probabilities. The RGB reading value ranges from 1 to 255.

Table 2. Red Odds

Range	Medium	High	*P*(*rse*)	*P*(*rti*)
1–63	0	0	0/68	0/132
64–127	66	6	66/68	6/132
128–190	0	127	0/68	127/132
191–255	0	1	0/68	1/132

Table 3. Green Odds

Range	Medium	High	*P*(*gse*)	*P*(*gti*)
1–63	0	0	0/68	0/132
64–127	66	120	66/68	120/132
128–190	0	14	0/68	14/132
191–255	0	0	0/68	0/132

Table 4. Blue Odds

Range	Medium	High	*P*(*bse*)	*P*(*bti*)
1–63	0	0	0/68	0/132
64–127	66	134	66/68	134/132
128–190	0	0	0/68	0/132
191–255	0	0	0/68	0/132

Example: The RGB value read by the sensor in the phosphorus meter:

$$x = \{R = 126; G = 111; B = 81\}. \quad (3)$$

Then, the phosphorus status of the rice fields is determined using Eq. (1).

The first step is to determine the probability of medium- and high-value $P(c)$ of all training data used for reading the paddy soil sample:

$$P(S) = 68/200; P(T) = 132/200. \quad (4)$$

Next, we determine the $P(x|c)$ value of the medium- and high-phosphorus-status probabilities of the known data classes:

Medium-phosphorus-status probability

$$P(rse) = 30/68; P(gse) = 68/68; P(bse) = 70/68. \quad (5)$$

High-phosphorus-status probability

$$P(rti) = 122/132; P(gti) = 70/132; P(bse) = 109/132. \quad (6)$$

For determining the $P(x|c)$ $P(c)$ value:

MEDIUM

$$P(c)P(se) = \frac{30}{68} \times \frac{68}{68} \times \frac{70}{68} \times \frac{68}{200} = 0.15. \quad (7)$$

HIGH

$$P(c)P(ti) = \frac{122}{132} \times \frac{70}{132} \times \frac{109}{132} \times \frac{132}{200} = 0.26. \quad (8)$$

The occurrence of the set probability value x in the entire data set is as follows:

$$P(x) = \frac{152}{200} \times \frac{138}{200} \times \frac{179}{200} = 0.58. \quad (9)$$

For determining the probabilities of moderate and high phosphorus status in the set value x, we proceed as follows:

$$\text{Moderate: } P(se|x) = \frac{0.15}{0.58} = 0.25; \quad (10)$$

$$\text{High: } P(ti|x) = \frac{0.26}{0.58} = 0.44. \quad (11)$$

So, the value $P(se|x) > P(ti|x)$.

It can be concluded that for RGB value

$$x = \{R = 126; G = 111; B = 81\} = Fosfor\ Tinggi. \quad (12)$$

The data obtained from the average RGB values of the 20 samples of paddy fields in Figure 6 that have been tested and classified using the Naïve Bayes algorithm are shown in Table 5.

Table 5 shows the average RGB values of all soils that were tested and classified using the Naïve Bayes algorithm. The classification results yielded seven moderate phosphorus statuses and 13 high phosphorus statuses.

A graph of the average RGB values of the test samples can be obtained from the classification results, as shown in Figure 7 for the 20 soil samples. Soils with medium phosphorus values are present in the 3rd, 4th, 10th, 11th, 12th, 17th, and 20th samples. High phosphorus values are indicated by the RGB values of the 1st, 2nd, 5th, 6th, 7th, 8th, 9th, 13th, 14th, 15th, 16th, 18th, and 19th samples.

3.3. Data Transfer to The *ceerduad.com* web

The data are sent to the *ceerduad.com* web server using the esp8266 WiFi module for sending the sensor reading data. The view of the ceerduad.com server is shown in Figure 8.

After successfully logging into the ceerduad.com website, a graph of the measurements of the paddy soil sample, which were read by the TCS3200 sensor, will be displayed according to the data that have been sent by the phosphorus-measuring instrument. The graphic image of the RGB value data that were successfully sent to the website is shown in Figure 9.

The graph in Figure 9 represents the sensor data sent from the phosphorus meter to the website based on the phosphorus meter reading. The graphic data in Figure 9 can be downloaded in Excel form. The graph shows the RGB values from the sampling at 20 rice fields in Lindahl District. Soil sample data are then extracted with PUTS and tested using a phosphorus meter that has been developed.

3.4. ArcGIS Mapping Design

Mapping is carried out to map the results of reading of the phosphorus levels in the soil samples at a specific location using several steps, as shown in Figure 10.

Table 5. Average RGB values of paddy fields

Sample	Average Red	Average Green	Average Blue	Status
1	149.5	128.1	91.3	High
2	146.2	128.3	91.4	High
3	110.7	95.5	72.2	Medium
4	123.6	107.8	77.0	Medium
5	130.8	110.3	78.4	High
6	134.5	115.0	82.2	High
7	144.3	124.2	87.6	High
8	145.3	126.7	92.1	High
9	138.8	119.4	85.8	High
10	119.9	103.7	76.9	Medium
11	118.7	103.4	75.1	Medium
12	120.5	103.2	75.9	Medium
13	148.9	125.7	87.7	High
14	134.3	112.3	80.3	High
15	139.2	115.1	79.1	High
16	139.2	113.9	79.9	High
17	122.8	103.4	72.4	Medium
18	143.0	119.2	85.4	High
19	132.4	109.0	75.8	High
20	110.5	93.9	67.0	Medium

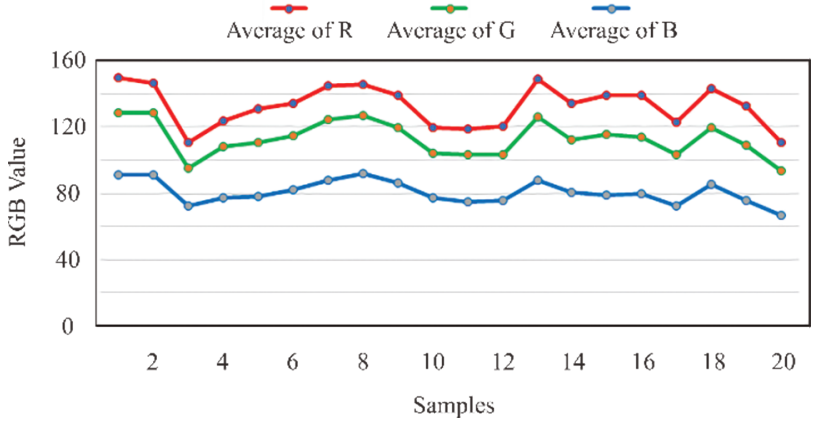

Figure 7: Chart Showing Average Value of Soil Phosphorus.

ArcGIS mapping was carried out by taking satellite imagery of the mapped location using Google Earth. The location pictures captured by the satellite are then used to create an SHP data (shapefile) map. The shapefile data that have been created are given an input of several attribute data scores, which then enter the stage of merging of several spatial elements into new spatial elements (overlay). The process of obtaining the cartographic map layout is completed in various steps, starting from the overlay process to

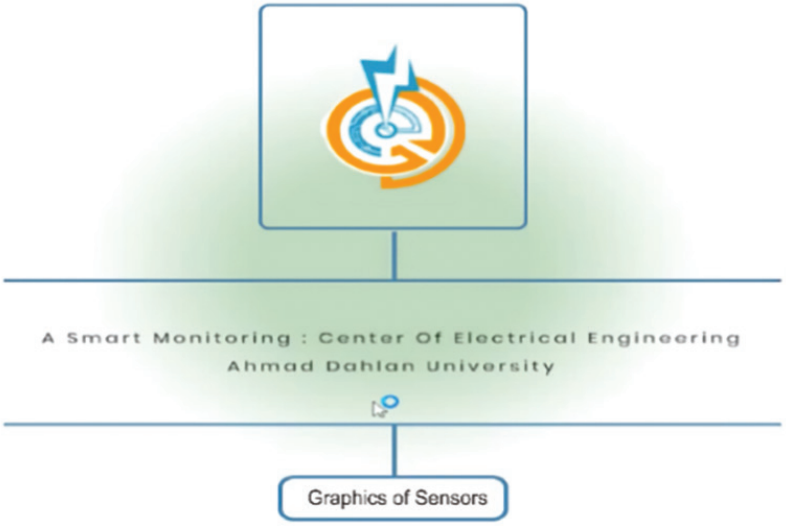

Figure 8: The first display of *ceerduaad.com* website.

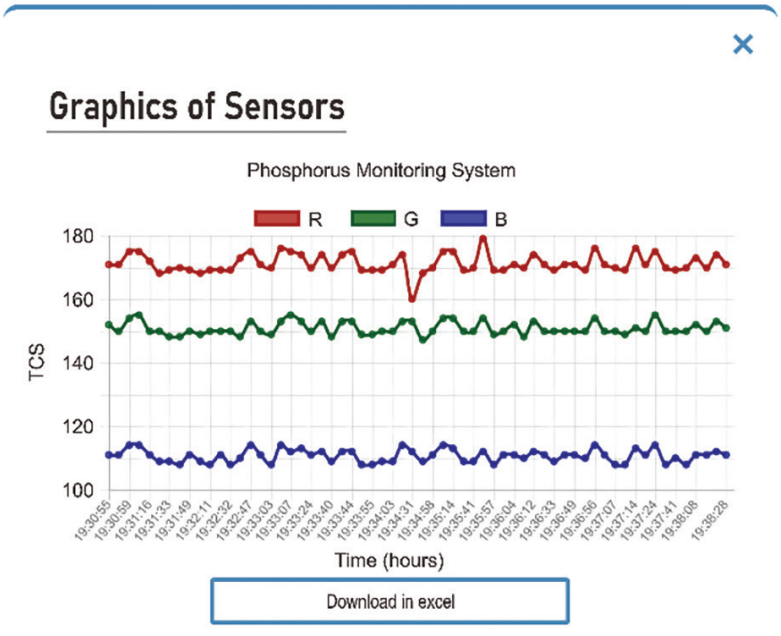

Figure 9: Graph displayed on the website.

the merging stage of several spatial elements into one spatial element without changing the combined spatial elements (union).

3.5. Paddy Soil Sampling Map

The sampling of paddy soil was carried out in the Lendah district, divided into 20 test locations, where each point represented one sample of paddy soil. The map of the paddy soil sampling distribution is shown in Figure 11.

ArcGIS software created a map of the sampling locations in Figure 11. ArcGIS is a processing software based on geographic data, which can present, manipulate, and save geographic information data. Some main features of the ArcGIS software in

mapping include the ArcMap and ArcCatalog. ArcMap is used in data management, including visualization, editing, and map-making, while ArcCatalog is a feature used for creating vector data, raster data, and grouping according to its function.

3.6. Paddy Soil Phosphorus Status Map

The mapping of the paddy fields' phosphorus status was accomplished based on the soil sampling location and phosphorus status obtained during the testing of the paddy soil samples, as shown in Figure 12.

From the mapping of the paddy soil phosphorus status in Figure 12, it can be seen that of the 20 locations of paddy soil sampling, 13 locations were of dark blue paddy fields and seven light blue locations. A dark blue indicator ▬ on the paddy soil phosphorus status map above indicates a high status of phosphorus, while the light blue color indicator ▬ on the map above indicates the moderate status of phosphorus.

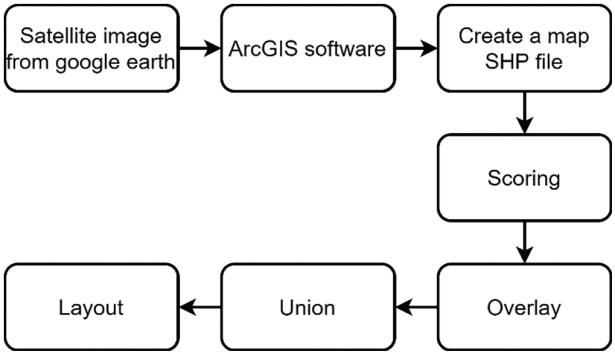

Figure 10: ArcGIS mapping diagram block.

3.7. Geographical Map of Soil Phosphorus Levels in Lendah District

This geographical map contains information that researchers prepared to facilitate use by readers, such as rivers, roads, village boundaries, inland waters, plantation villages, and rice fields. This map aims to focus on the nutrient content in terms of soil phosphorus in the rice fields of Lendah district. The final result of mapping of phosphorus levels in the Lendah District is shown in Figure 13.

In making the phosphorus content map, Figure 13 used the raster and vector data. Raster data is in the form of squares or cells. Raster data like a image data presented in the form of jpg and unitary coordinates in square. Vector data are in the form of spatial data such as points, lines, and areas. On a map, raster data form an image in jpg format, while vector data are in the form of roads, rivers, village boundaries (in the form of lines), villages, and rice fields (data that have a large area).

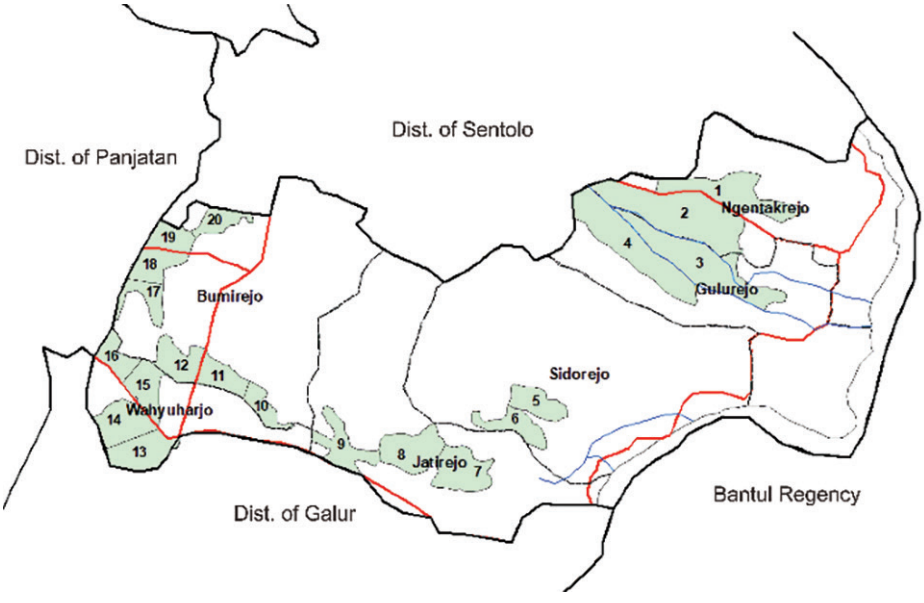

Figure 11: A map of the paddy soil sampling locations.

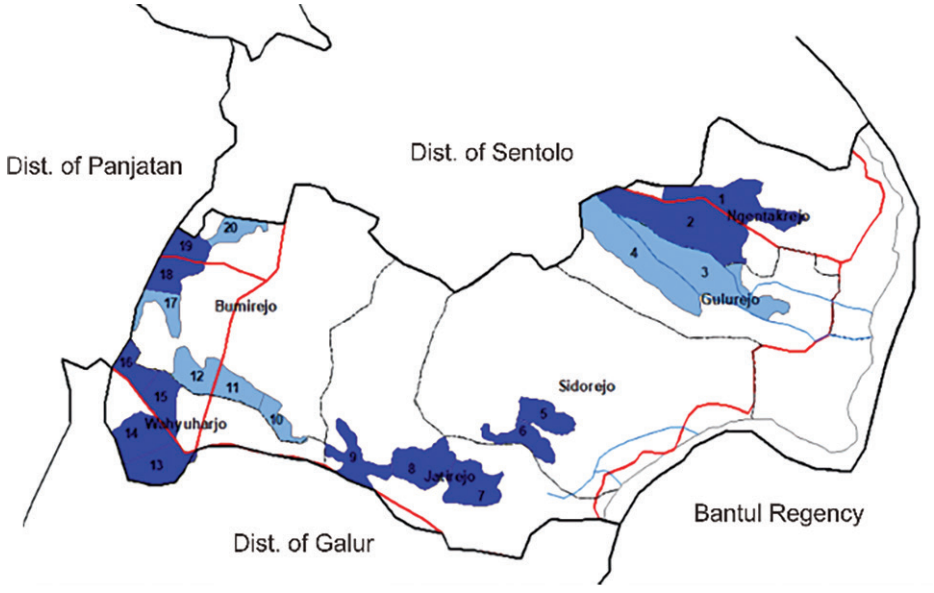

Figure 12: Paddy soil phosphorus status map based on the sampling location.

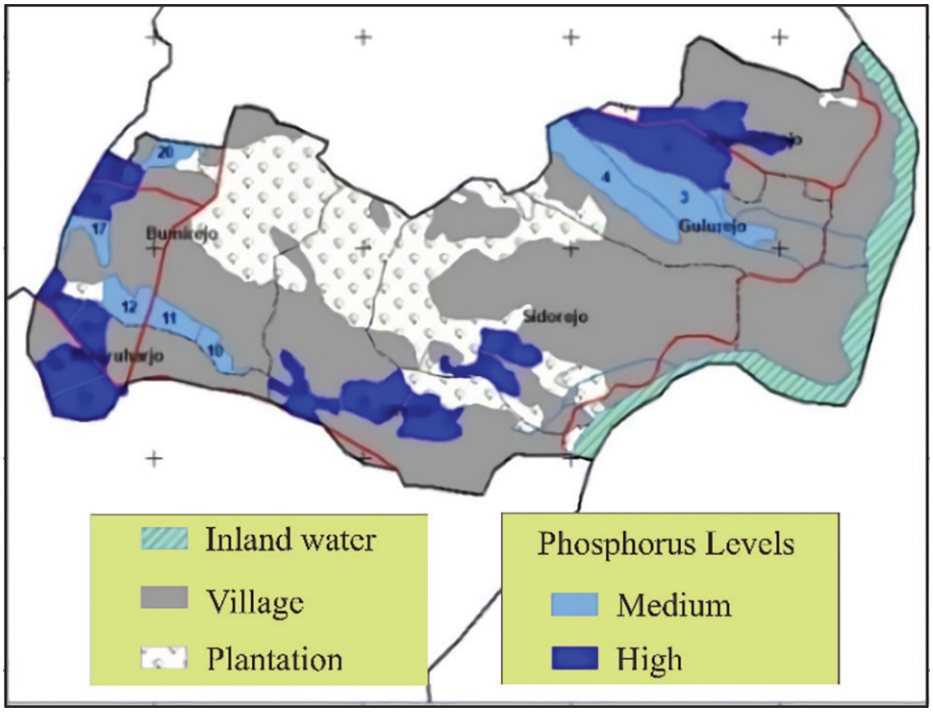

Figure 13: Map of Paddy Soil Phosphorus Levels in Lendah District.

4. Conclusion

Based on the results of testing with the developed tools, we can conclude that the paddy soil phosphorus-level measurement tool can measure the paddy soil phosphorus status with an error rate of 3%, and the success rate reaches 97%. The RGB values of the 20 paddy soil samples in Lendah District

with 200 readings of the phosphorus-measuring instrument showed medium and high phosphorus statuses in the soil samples taken. The weakness of the Naïve Bayes algorithm in this study is that if one of the variables used is zero, then it is final the result of the data obtained will be zero. Even if only one data point is worth zero, all data will be affected. An alternative solution to overcome the drawbacks of using the Naïve Bayes method can be modified with the Laplacian correction algorithm to avoid the probability value of zero.

Acknowledgments

The researchers thank the Institute of Research and Community Services (LPPM) for facilitating this research and the respondents who were involved in this research.

Funding

The authors received no financial support for this research, authorship, and publication of this article.

Competing Interests

The authors have stated no conflict of interest.

Authors' Contributions

Anton Yudhana: Supervision. Andreyan Dwi Cahyo: Investigation, collection of data, and implementation of computer code. Liya Yusrina Sabila: Conceptualization and formal analysis, application of statistics, and provision of study material. Arsyad Cahya Subrata: Validation, software development, and designing of the computer program. Ilham Mufandi: Project administration, writing, editing, visualization, resources, and original draft.

References

[1] M. A. Arham, A. Fadhli, and S. I. Dai, "Does Agricultural Performance Contribute to Rural Poverty Reduction in Indonesia?" *Jejak*, vol. 13, no. 1, pp. 69–83, 2020, doi: 10.15294/jejak.v13i1.20178.

[2] E. Loizou, C. Karelakis, K. Galanopoulos, and K. Mattas, "The role of agriculture as a development tool for a regional economy," *Agric. Syst.*, vol. 173, no. April, pp. 482–490, 2019, doi: 10.1016/j.agsy.2019.04.002.

[3] N. Sauqi, A. A. Sigit, and J. Jumadi, "The Analysis Impact of Irrigation Channel on Rice Production in Bendosari, Sukoharjo Regency," *Int. J. Disaster Dev. Interface*, vol. 1, no. 1, pp. 1–8, 2021, doi: 10.53824/ijddi.v1i1.5.

[4] C. Wang, P. Ghadimi, M. K. Lim, and M. L. Tseng, "A literature review of sustainable consumption and production: A comparative analysis in developed and developing economies," *J. Clean. Prod.*, vol. 206, no. 01, pp. 741–754, 2019, doi: 10.1016/j.jclepro.2018.09.172.

[5] L. B. Sejati, Y. Arifien, and F. Maad, "Economic valuation of rice agricultural land in Bogor regency," *J. Phys. Conf. Ser.*, vol. 1517, no. 1, 2020, doi: 10.1088/1742-6596/1517/1/012024.

[6] A. T. Braun, E. Colangelo, and T. Steckel, "Farming in the Era of Industrie 4.0," *Procedia CIRP*, vol. 72, pp. 979–984, 2018, doi: 10.1016/j.procir.2018.03.176.

[7] A. Yudhana and A. C. Kusuma, "Water quality monitoring at paddies farming based on android," *IOP Conf. Ser. Mater. Sci. Eng.*, vol. 403, no. 1, 2018, doi: 10.1088/1757-899X/403/1/012042.

[8] A. Yudhana, Y. D. Andriliana, S. A. Akbar, Sunardi, S. Mukhopadhyay, and I. R. Karas, "Monitoring of rainfall level ombrometer observatory (Obs) type using android sharp GP2Y0A41SK0F sensor," *Int. J. Adv. Comput. Sci. Appl.*, vol. 10, no. 11, pp. 360–364, 2019, doi: 10.14569/IJACSA.2019.0101150.

[9] A. Yudhana, J. Rahmayanti, S. A. Akbar, S. Mukhopadhyay, and I. R. Karas, "Modification of manual raindrops type observatory ombrometer with ultrasonic sensor HC-SR04," *Int. J. Adv. Comput. Sci. Appl.*, vol. 10, no. 12, pp. 277–281, 2019, doi: 10.14569/ijacsa.2019.0101238.

[10] A. Yudhana, R. Umar, and F. M. Ayudewi, "The Monitoring of Corn Sprouts Growth Using the Region Growing Methods," *J. Phys. Conf. Ser.*, vol. 1373, no. 1, 2019, doi: 10.1088/1742-6596/1373/1/012054.

[11] A. Yudhana, Sunardi, and S. Saifullah, "Segmentation comparing eggs watermarking image and original image," *Bull. Electr. Eng. Informatics*, vol. 6, no. 1, pp. 47–53, 2017, doi: 10.11591/eei.v6i1.595.

[12] L. Guo et al., "Using aquatic animals as partners to increase yield and maintain soil nitrogen in the paddy ecosystems," *Elife*, vol. 11, pp. 1–30, 2022, doi: 10.7554/elife.73869.

[13] M. F. Stuecker, M. Tigchelaar, and M. B. Kantar, "Climate variability impacts on rice production in the Philippines," *PLoS One*, vol. 13, no. 8, pp. 1–17, 2018, doi: 10.1371/journal.pone.0201426.

[14] M. Spohn and P. M. Schleuss, "Addition of inorganic phosphorus to soil leads to desorption of organic compounds and thus to increased soil

respiration," *Soil Biol. Biochem.*, vol. 130, pp. 220–226, 2019, doi: 10.1016/j.soilbio.2018.12.018.

[15] K. A. Jarosch, E. Kandeler, E. Frossard, and E. K. Bünemann, "Is the enzymatic hydrolysis of soil organic phosphorus compounds limited by enzyme or substrate availability?" *Soil Biol. Biochem.*, vol. 139, p. 107628, 2019, doi: 10.1016/j.soilbio.2019.107628.

[16] J. Kazmierczak et al., "Groundwater-controlled phosphorus release and transport from sandy aquifer into lake," *Limnol. Oceanogr.*, vol. 65, no. 9, pp. 2188–2204, 2020, doi: 10.1002/lno.11447.

[17] H. Lambers, "Annual Review of Plant Biology Phosphorus Acquisition and Utilization in Plants Measuring Plant Respiration using stable isotopes of oxygen View project SoilCare View project Phosphorus Acquisition and Utilization in Plants," *Artic. Annu. Rev. Plant Biol.*, no. January, 2022, doi: 10.1146/annurev-arplant-102720-CITATIONS.

[18] K. D. Schneider et al., "Options for Improved Phosphorus Cycling and Use in Agriculture at the Field and Regional Scales," *J. Environ. Qual.*, vol. 48, no. 5, pp. 1247–1264, 2019, doi: 10.2134/jeq2019.02.0070.

[19] Y. K. Kalkhajeh et al., "Methods for sample collection, storage, and analysis of freshwater phosphorus," *Water (Switzerland)*, vol. 11, no. 9, pp. 1–24, 2019, doi: 10.3390/w11091889.

[20] H. Malhotra, Vandana, S. Sharma, and R. Pandey, "Phosphorus Nutrition: Plant Growth in Response to Deficiency and Excess," *Plant Nutr. Abiotic Stress Toler.*, no. July, pp. 1–590, 2018, doi: 10.1007/978-981-10-9044-8.

[21] C. Alewell, B. Ringeval, C. Ballabio, D. A. Robinson, P. Panagos, and P. Borrelli, "Global phosphorus shortage will be aggravated by soil erosion," *Nat. Commun.*, vol. 11, no. 1, 2020, doi: 10.1038/s41467-020-18326-7.

[22] Y. Wang, Y. F. Chen, and W. H. Wu, "Potassium and phosphorus transport and signaling in plants," *J. Integr. Plant Biol.*, vol. 63, no. 1, pp. 34–52, 2021, doi: 10.1111/jipb.13053.

[23] A. Kumar, A. Kumar, and H. Patel, "Role of Microbes in Phosphorus Availability and Acquisition by Plants," *Int. J. Curr. Microbiol. Appl. Sci.*, vol. 7, no. 05, pp. 1344–1347, 2018, doi: 10.20546/ijcmas.2018.705.161.

[24] C. J. Penn and J. J. Camberato, "A critical review on soil chemical processes that control how soil ph affects phosphorus availability to plants," *Agric.*, vol. 9, no. 6, pp. 1–18, 2019, doi: 10.3390/agriculture9060120.

[25] T. B. H. Zulkifli and Y. Hasanah, "Growth and yield characteristics of soybean on the usage of several varieties and fertilizers N, P, K in tidal lowland," *IOP Conf. Ser. Earth Environ. Sci.*, vol. 782, no. 4, 2021, doi: 10.1088/1755-1315/782/4/042038.

[26] P. Sanjeevi, S. Prasanna, B. Siva Kumar, G. Gunasekaran, I. Alagiri, and R. Vijay Anand, "Precision agriculture and farming using Internet of Things based on wireless sensor network," *Trans. Emerg. Telecommun. Technol.*, vol. 31, no. 12, pp. 1–14, 2020, doi: 10.1002/ett.3978.

[27] K. S. Lubis, Supriadi, M. J. Sibarani, and A. Z. Siregar, "Jurnal Pertanian Tropik Jurnal Pertanian Tropik," *Surv. Mapp. P Nutr. Status Paddy L. Aek Simare Irrig. Area, Laguboti Dist. Toba Samosir Regency, North. Sumatera, Indones.*, vol. 7, no. 1, 2020, doi: https://doi.org/10.32734/jpt.v7i1,April.3821.

[28] J. Devare and N. Hajare, "A Survey on IoT Based Agricultural Crop Growth Monitoring and Quality Control," *Proc. 4th Int. Conf. Commun. Electron. Syst. ICCES 2019*, pp. 1624–1630, 2019, doi: 10.1109/ICCES45898.2019.9002533.

[29] A. Gholizadeh, M. Saberioon, E. Ben-Dor, and L. Borůvka, "Monitoring of selected soil contaminants using proximal and remote sensing techniques: Background, state-of-the-art and future perspectives," *Crit. Rev. Environ. Sci. Technol.*, vol. 48, no. 3, pp. 243–278, 2018, doi: 10.1080/10643389.2018.1447717.

[30] K. T. E. Keerthana, S. Karpagavalli, and A. Mary Posonia, "Smart system monitoring agricultural land using Iot," *2018 Int. Conf. Emerg. Trends Innov. Eng. Technol. Res. ICETIETR 2018*, pp. 1–7, 2018, doi: 10.1109/ICETIETR.2018.8529037.

[31] Arvin N. Natividad; Luisito L. Lacatan, "Solar-Powered Soil Nutrient Detector for Rice Field," *Test Eng. Manag.*, vol. 82, no. February 2020, pp. 4267–4276, 2020.

[32] M. A. E. AbdelRahman, A. Shalaby, and E. S. Mohamed, "Comparison of two soil quality indices using two methods based on geographic information system," *Egypt. J. Remote Sens. Sp. Sci.*, vol. 22, no. 2, pp. 127–136, 2019, doi: 10.1016/j.ejrs.2018.03.001.

[33] G. Lü, M. Batty, J. Strobl, H. Lin, A. X. Zhu, and M. Chen, "Reflections and speculations on the progress in Geographic Information Systems (GIS): a geographic perspective," *Int. J. Geogr. Inf. Sci.*, vol. 33, no. 2, pp. 346–367, 2019, doi: 10.1080/13658816.2018.1533136.

[34] H. Kazemi and H. Akinci, "A land use suitability model for rainfed farming by Multi-criteria Decision-making Analysis (MCDA) and Geographic Information System (GIS)," *Ecol. Eng.*, vol. 116, no. March, pp. 1–6, 2018, doi: 10.1016/j.ecoleng.2018.02.021.

[35] A. Sathish, B. K. Ramachandrappa, K. Devaraja, M. S. Savitha, M. N. Thimme Gowda, and K. M. Prashanth, "Assessment of spatial variability in fertility status and nutrient recommendation in Alanatha Cluster villages, Ramanagara district, Karnataka using GIS," *J. Indian Soc. Soil Sci.*, vol. 66, no. 2, pp. 149–157, 2018, doi: 10.5958/0974-0228.2018.00019.1.

[36] G. Ayalew, "A Geographic Information System Based Physical Land Suitability Evaluation to Groundnut and Sweet Potato in East Amhara, Highlands of Ethiopia," *Citeseer*, vol. 5, no. 1, pp. 33–39, 2015.

[37] Rahmawaty, S. Frastika, A. Rauf, R. Batubara, and F. S. Harahap, "Land suitability assessment for Lansium domesticum cultivation on agroforestry land using matching method and geographic information system," *Biodiversitas*, vol. 21, no. 8, pp. 3683–3690, 2020, doi: 10.13057/biodiv/d210835.

[38] M. Masoudi, P. Jokar, and E. Ramezanipour, "A GIS-based quantitative model for land use planning in Larestan County, Iran," *Eqa-International J. Environ. Qual.*, vol. 40, pp. 19–30, 2020, doi: 10.6092/issn.2281-4485/10433.

[39] B. Bolo, D. Mpoeleng, and I. Zlotnikova, "Geospatial information system land evaluation analysis for rainfed farming using multi-criteria decision analysis approach," *J. Agric. Informatics*, vol. 9, no. 3, 2018, doi: 10.17700/jai.2018.9.3.472.

[40] W. Chen, S. Zhang, R. Li, and H. Shahabi, "Performance evaluation of the GIS-based data mining techniques of best-first decision tree, random forest, and naïve Bayes tree for landslide susceptibility modeling," *Sci. Total Environ.*, vol. 644, pp. 1006–1018, 2018, doi: 10.1016/j.scitotenv.2018.06.389.

[41] B. T. Pham and I. Prakash, "A novel hybrid model of Bagging-based Naïve Bayes Trees for landslide susceptibility assessment," *Bull. Eng. Geol. Environ.*, vol. 78, no. 3, pp. 1911–1925, 2019, doi: 10.1007/s10064-017-1202-5.

[42] F. Ikorasaki and M. B. Akbar, "Detecting Corn Plant Disease with Expert System Using Bayes Theorem Method," *2018 6th Int. Conf. Cyber IT Serv. Manag. CITSM 2018*, no. Citsm, pp. 1–3, 2019, doi: 10.1109/CITSM.2018.8674303.

[43] S. Lee, M. J. Lee, H. S. Jung, and S. Lee, "Landslide susceptibility mapping using Naïve Bayes and Bayesian network models in Umyeonsan, Korea," *Geocarto Int.*, vol. 0, no. 0, p. 000, 2019, doi: 10.1080/10106049.2019.1585482.

[44] A. Yudhana, D. Sulistyo, and I. Mufandi, "GIS-based and Naïve Bayes for nitrogen soil mapping in Lendah, Indonesia," *Sens. Bio-Sensing Res.*, vol. 33, p. 100435, 2021, doi: 10.1016/j.sbsr.2021.100435.

[45] H. Kurniadi Wardana, E. Indahwati, and L. Arifah Fitriyah, "Measurement of Non-Invasive Blood Glucose Level Based Sensor Color TCS3200 and Arduino," *IOP Conf. Ser. Mater. Sci. Eng.*, vol. 336, no. 1, 2018, doi: 10.1088/1757-899X/336/1/012019.

[46] S. Dwiasnati and Y. Devianto, "Naïve Bayes Optimization Based On Particle Swarm Optimization to Predict the Decision of Insurance Customer Candidate," *Int. J. Comput. Tech.*, vol. 5, no. 5, pp. 8–14, 2018, doi: 10.29126/23942231/IJCT-V5I5P2.

[47] R. Priya, D. Ramesh, and E. Khosla, "Crop Prediction on the Region Belts of India: A Naïve Bayes MapReduce Precision Agricultural Model," *2018 Int. Conf. Adv. Comput. Commun. Informatics, ICACCI 2018*, pp. 99–104, 2018, doi: 10.1109/ICACCI.2018.8554948.

[48] S. Al Irfan, A. Yudhana, S. C. Mukhopadhyay, I. R. Karas, D. E. Wati, and I. Puspitasari, "Wireless Communication System for Monitoring Heart Rate in the Detection and Intervention of Emotional Regulation," *Proc. - 1st Int. Conf. Informatics, Multimedia, Cyber Inf. Syst. ICIMCIS 2019*, pp. 243–248, 2019, doi: 10.1109/ICIMCIS48181.2019.8985210.

[49] L. He et al., "Angular effect of algorithms for monitoring leaf nitrogen concentration of wheat using multi-angle remote sensing data," *Comput. Electron. Agric.*, vol. 195, no. January, 2022, doi: 10.1016/j.compag.2022.106815.

[50] Y. Zhuang et al., "Real-time measurement of total nitrogen for agricultural runoff based on multiparameter sensors and intelligent algorithms," *Water Res.*, vol. 210, no. December 2021, p. 117992, 2022, doi: 10.1016/j.watres.2021.117992.

[51] A. Fadlil, I. Riadi, and S. Aji, "DDoS Attacks Classification using Numeric Attribute-based Gaussian Naïve Bayes," *Int. J. Adv. Comput. Sci. Appl.*, vol. 8, no. 8, pp. 42–50, 2017, doi: 10.14569/ijacsa.2017.080806.

[52] M. Muthmainnah, M. Ashar, I. M. Wirawan, and T. Widiyaningtyas, "Time Series Forecast for Rainfall Intensity in Malang City with Naïve Bayes Methodology," *3rd Int. Conf. Sustain. Inf. Eng. Technol. SIET 2018 - Proc.*, pp. 137–141, 2018, doi: 10.1109/SIET.2018.8693171.

[53] J. Segarra, et al., "Multiscale assessment of ground, aerial and satellite spectral data for monitoring wheat grain nitrogen content," *Information Processing in Agriculture.*, 2022, doi: 10.1016/j.inpa.2022.05.004.